MASTER
FILE COPY
BUREAU OF RECLAMATION
HYDRAULIC LABORATORY
NOT TO BE REMOVED FROM FILES

HYD 95

UNITED STATES
DEPARTMENT OF THE INTERIOR
BUREAU OF RECLAMATION

- - -

HYDRAULIC LABORATORY REPORT NO. HYD-95

HYDRAULIC MODEL STUDIES OF GREEN MOUNTAIN PENSTOCK

- - -

HYDRAULIC MACHINERY LABORATORY
REPORT NO. HM-6

- - -

Denver, Colorado
June, 1941

Bureau of Reclamation

Hydraulic Machinery Laboratory

Denver, Colorado
February , 1941

Laboratory Report No. HM-6
Green Mountain Dam
Colo.-Big Thompson Project
Compiled by: W. A. Hamilton
O. S. Hanson
Checked by: D. J. Hebert
Submitted by G. J. Hornsby

Subject: Hydraulic model studies of Green Mountain penstock.

1. Introduction. Green Mountain Dam is a part of the Colorado-Big Thompson project and its purpose is to store the flood flow of the Blue River and release this water to the Colorado River at a rate which will offset the effect of the diversion of water from Grand Lake through the Continental Divide tunnel. This storage and release of water will require a drawdown in Green Mountain reservoir of 135 feet each year in advance of the flood season.

Two 15,000-horsepower turbines and two 50-inch outlet valves will be installed in Green Mountain power plant. Each turbine will be supplied with water by a 102-inch diameter penstock. The penstock system which supplies the turbines and auxiliary outlet valves consists of a trashrack structure at the intake, a concrete-lined inlet shaft 15 feet 5 inches in diameter, a concrete-lined tunnel 18 feet in diameter and approximately 810 feet long extending from the inlet shaft to a gate chamber where the flow is divided and passed through two 102-inch ring-seal gates connected to 102-inch steel penstocks installed in a concrete-lined, horseshoe-shaped tunnel approximately 710 feet long. Y-branches located upstream from the powerhouse divert all or a portion of the flow to the 50-inch outlet valves. The principal features of the penstock system are shown in figure 1.

2. Summary. Models of several elbow designs were tested to determine the most efficient one for installation at Green Mountain Dam. The most efficient one is an elbow of constant diameter with a radius of curvature of one and one-half diameters followed by a minimum length of one and one-half diameters of straight pipe before flaring to the tunnel diameter.

It was found that the piers and trash-rack bars are essential in preventing the formation of vortices at minimum reservoir level. However, the shape of the pier itself has very little effect, and it is suggested that structural considerations be the basis for selection of pier shape.

Three designs of Y-branches were studied and it was found that the straight Y has minimum loss at zero diversion whereas the conical Y has minimum loss at 100 percent diversion. Since the difference in these two is very small at low diversions, the conical Y is the

better design, considering all conditions of operation.

3. Purpose of studies. The hydraulic model study was undertaken initially for the purpose of selecting the most efficient design of bend which would satisfy design requirements.

When the bend studies were completed, it was decided that a study of entrance conditions at minimum water surface should be made because of the possibility that vortices might form and draw air into the turbine penstock.

In order to supply hydraulic design information, three Y-branch designs, including a new type with vanes, were tested.

4. Experimental apparatus and test procedure. A model of the structure from the bellmouth entrance to a point about 60 diameters downstream from the elbow was constructed to a scale of 1:29.671. This model ratio was chosen so that available materials could be used. The reservoir was simulated by a metal-lined wooden box of ample size to insure proper performance of the entrance. The bellmouth entrance was machined from a bronze casting to the shape recommended in Laboratory Report No. HM-1 of the Hydraulic Machinery Laboratory, Bureau of Reclamation. From this point to a point 34 diameters downstream from the bend, the model, including the various elbow models, was made of transparent pyralin to allow visual observation of flow conditions. The remaining portion of the model consisted of an aluminum pipe 7.19 inches in diameter. An orifice 6-1/2 inches in diameter was placed at the end of this pipe to partially restrict the flow.

Water was delivered to the head box through suitable piping by an 8-inch centrifugal pump, and, after passing through the model, it emptied into a tank which had a sharp-edged orifice in one side. This tank was equipped with sufficient baffles to give proper flow conditions for the orifice. A water column connected to the tank served to indicate the head over the orifice.

5. Elbow tests. In testing the various elbow models no attempt was made to maintain operational similitude. It was decided that the performance of the various designs be compared on the basis of the discharge under the same head. In order to obtain significant differences in discharge for the various elbows, the model setting was designed for the maximum capacity of the circulating pump. The resulting velocities were several times the velocity scaled from the prototype. This distortion of the velocity scale resulted in an increase in Reynolds' number which makes the tests more truly indicative of the prototype behavior. An orifice was chosen to measure discharge because of its relatively high sensitivity to change in discharge.

The testing procedure followed a simple pattern. The discharge

of the pump was adjusted until the level in the head box reached a predetermined level. With the head at this level, the discharge was measured by means of the orifice box at the end of the model. The level in the head box and the head over the measuring orifice were read simultaneously at 15-second intervals for a total of ten readings on each. It was very difficult to set the level in the head box at the exact level desired; so a set of ten readings was taken slightly above and one slightly below this level. The discharge at the desired head was then obtained by interpolation.

These discharge tests were run in succession and in as short a time as possible so that all the elbows were tested under nearly identical conditions. After completing the entire set in this manner, each elbow was installed again and the following additional tests were made.

The velocity distribution at critical sections was obtained by means of a cylindrical pitot tube. This tube has three openings in a plane perpendicular to its axis. These three openings are connected to manometers which are read to give the magnitude and direction of the velocity vector in the plane of the holes. The direction is obtained directly by balancing the pressures on the outside holes, and the magnitude is computed from the differential between the center hole and either of the outside ones. Measurements were taken across two diameters at right angles to each other. At the same time, the energy loss was obtained by reading the differential head between the center hole and the headwater.

Pressure measurements were taken at several sections, including all sections where velocity traverses were made. These pressures were obtained by means of piezometer rings connected to water or mercury columns, depending on the magnitude of the pressure.

6. Intake tests. A few changes had to be made in the model for the intake studies. Whereas in the elbow studies, which were strictly comparative, the discharge scale could be ignored, such is not the case for the intake studies. In studying the vortex conditions at the intake for a definite head over the entrance, it is essential that the discharge be in the correct ratio to this head. To accomplish this the 6-1/2-inch orifice at the end of the aluminum pipe was replaced by a smaller orifice, 2.52 inches in diameter, which gave the scaled head at the scaled discharge. In other words, operational similitude was maintained. The smaller orifice represents the control of the system maintained by the turbine. All the intake tests were visual and consisted of trying various shapes of piers and a training wall of special design. The model structure is shown in plate 1.

7. Y-branch tests. After concluding the elbow and intake

tests, the aluminum pipe was replaced by a sheet-metal pipe of equal diameter flanged so that the Y-branch models could be placed between the pyralin and sheet-metal pipes. The entire model, including the headwater box, was moved to a new location under an elevated V-notch weir box so that the water could be metered as it entered the model. A free discharge orifice was installed at the end of the sheet-metal pipe to measure the discharge through this line. The difference between the discharge measured by the V-notch weir and that measured by the orifice gave the discharge diverted through the branch.

A valve at the end of the branch line served to control the percentage of total flow diverted by the branch within the limits of the ratio set by the size of the orifice at the end of the direct pipe. This ratio was varied by changing the size of the discharge orifice. For 100 percent diversion the direct line was blanked off.

In testing the Y-branch models, operational similitude was again disregarded and maximum model discharge was used. The level in the headwater box was held as high as possible and the total discharge over the V-notch (Q_t) and the discharge through the orifice (Q_d) were measured. Pressure readings were taken at four sections, located as shown in figure 6, by means of ring piezometers and manometer tubes. Some velocity traverses were also taken at these sections.

8. Results and conclusions.

Elbows.--The elbows tested were all 90-degree bends and had approximately the same radius of curvature, 9.302 inches in the model, with the exception of the long radius and vaned elbows. The design of each elbow tested, as well as the location of the measuring sections, is shown in figures 2, 3, and 4. The results of the comparative discharge tests are shown in the following table. Each elbow is listed according to the value of the measured discharge adjusted to the same head.

Bend No.	Description of Elbow	Discharge, c.f.s.	
3	Long radius	3.114	3.115
8	Constant diameter - 1-1/2 D straight	3.077	3.073
8A	Constant diameter - 2-1/2 D straight	3.070	3.071
9	Converging-elliptical	3.040	3.037
5	Constant diameter - with throat	3.018	3.018
9A	Converging-elliptical - 1-1/2 D straight	3.000	3.002
1	Converging-double conical	2.989	2.988

Bend No.	Description of Elbow	Discharge, c.f.s.	
7	Converging-single conical	2.988	2.985
6	Constant diameter-no straight	2.982	2.976
4A	Vanes - 5 vanes	2.972	2.971
2	Converging - spiral, elliptical	2.940	2.938
4	Vanes - 9 vanes	2.901	2.901

The foregoing table gives a comprehensive picture of the comparative performance of the various elbows. It will be noted that two discharges are listed for each elbow arrangement. The first discharge listed is the value obtained directly from the tests by interpolation, as explained previously. In obtaining these values the variation in the length of the elbows was neglected. Any variation in this length results in the same variation in over-all length of the model because all other model lengths were fixed. In order that the results be strictly comparable, this change was corrected by adding a hypothetical length of 7.2-inch diameter pipe of sufficient length to compensate for the variations. The loss in this added length was computed by proportion from the measured loss in 23.4 diameters of 7.2-inch diameter pipe downstream from the long radius elbow. The decrease in discharge resulting from this additional loss with the same total head was then computed by the relation:

$$Q(\text{corrected}) = Q(\text{measured}) \times \sqrt{\frac{K}{K + c}}$$

where

$$K = H(\text{total}) / \frac{V^2}{2g} \quad \text{and} \quad V = Q(\text{meas.})^2 / A^2$$

and

$$c = h / \frac{V^2}{2g}, \text{ where } h = \text{loss in added length.}$$

The corrected values of discharge do not differ materially from the uncorrected values except in the case of elbow No. 6 where the change amounts to two-thirds of a percent. No changes occur in the relative performance of the elbows due to the correction. An interesting point is revealed for the case of the constant diameter elbow with the two different lengths of tangent. Although frictional loss is increased by adding the length of smaller pipe for the longer tangent, the net effect is only a slight lowering in discharge. This is undoubtedly due to an offsetting increase in the efficiency of the diffuser. There is an optimum length of tangent, but no attempt was made to find it because the change in performance of the elbows is very slight. It can be stated that the length of the tangent is not critical between 1-1/2 and 2-1/2 diameters, and the final design can

be any length between these two values.

The results indicate that the long radius elbow, which has the generally recognized optimum ratio of radius to diameter of 4 to 1, is the most efficient elbow. This elbow was included in the tests merely as a ma tter of control, since the choice of elbow design is limited by design conditions to one of short radius, which could be formed within the diversion tunnel plug. The most efficient elbow for installation is then a constant-diameter elbow with a radius of 1-1/2 diameters and a length of downstream tangent equal to a minimum of 1-1/2 diameters.

In selecting the elbow for Green Mountain Dam penstock it was unnecessary to consider velocity distribution because of the long run of pipe between the elbow and the turbines. However, measurements of velocity distribution were taken to complete the test of each elbow. These tests are included and discussed for consideration in future designs. The velocity at any point in a section was obtained from the differentials measured with the cylindrical pitot tube by means of the relationship $V^2/2g = Kh$. The coefficient K had been evaluated in previous tests by traversing a pipe with a known discharge passing.

The results of these velocity studies are shown in figures 2, 3, and 4. A sketch of each elbow shows its design and the locations of the measuring sections. The velocity distribution at each section is shown in two ways; first, by means of isotachs drawn on the cross section, and, second, by nondimensional plots of velocity versus distance from the side. The cross sections with the isotachs show the manner in which the distribution changes around each elbow. The nondimensional plots give a comparison of distribution at each section for different elbows.

These plots of velocity distribution give a comprehensive picture of the conditions to be expected downstream from the elbows of the types tested. For the specific study which is the subject of this report, the distribution of velocity is of no consequence. However, there are many installations where the distribution is important. It is apparent from a study of these plots that the distribution is materially the same at section 6 for all the elbows. This section is located at a distance of 7.4 diameters of the 7.2-inch pipe plus some 4 diameters of the 6.235-inch pipe from the center line of the vertical pipe. This distance, together with the fact that a diffuser preceded this section, accounts for the relative invariance of the velocity distribution. At sections which are located closer to the elbow, the distributions are quite different for the various elbows. The vaned elbow is clearly superior to all the others from the standpoint of distribution. The accelerating elbows are fair up to the

minimum section but from here on the distribution becomes distorted in a short distance and then gradually improves up to section 6. It is apparent that so long as the water is being accelerated, the flow remains stable and well distributed, but as soon as the acceleration is stopped, secondary flow develops. The secondary flow actually develops before the end of acceleration is reached.

It has been contended that if any acceleration feature is imposed on a bend it should be placed downstream from the bend and separate from it. These tests seem to bear out this contention. With the exception of bend No. 9, the constant diameter elbow followed by a nozzle is the most efficient of the acceleration bends. Since the amount of acceleration is materially less for the case of bend No. 9, it cannot be compared directly with the other acceleration bends.

The nondimensional plots serve to compare the flow at any section for different elbows. A few of the traverses are somewhat in error, due to the influence of the measuring tube. This is the case only for the smaller sections where the cross-sectional area of the tube is relatively large. The superiority of the vaned-type elbow is again demonstrated in these plots.

Intake.—Since all the piers tested had the same shape of tail, the model was built with that part of the pier fixed in place, with facilities for changing the nose pieces. The various pier shapes tested, as well as the curved training wall, are shown in figure 5.

The intake model was first operated without any trashrack structure. Small eddies combined to form a large vortex which drew in an undesirable quantity of air. The piers were then installed. The presence of the piers reduced the vortex action to a large extent. Although small vortices continued to form over the intake, they were held to such a size by the piers that air was drawn in only at intervals and then only a few bubbles. The action was as follows. A small eddy would form at the side of a pier and then drift in over the intake. This eddy would grow in size until it was suddenly damped out by the piers. When the trashracks were installed the tendency to form vortices was again reduced. The presence of the trashrack bars prevented the formation of the eddies at the side of the piers which, in the previous set-up, led to a vortex over the intake. A number of small eddies was created behind the trashrack bars but they seemed to be distributed at random so that they acted to compensate each other. With regard to the action of the different pier-nose designs, no marked difference could be detected by visual observation. A larger orifice, 4 inches in diameter, was substituted for the 2.52-inch orifice at the end of the model in order to increase the flow through the model and thereby magnify any differences. There was still no appreciable difference in the flow characteristics. No attempt was made to measure losses because they are of such small magnitude that

they were almost imperceptible in the model. The choice of pier nose is therefore one dictated by structural considerations. The training wall was then installed and studied. The presence of this wall contributed no appreciable improvement in flow conditions.

In all cases vortices formed over the intake, but with the piers and trashrack bars in place the vortices were small and only occasionally reached the size necessary to take in air. There is definitely no large single vortex such as formed over the intake without piers and trashrack bars.

In order to stop all vortex formation it would be necessary to drop the bulkhead gate and allow it to float on the surface when the water level is low.

Y-branch.--The Y-branch studies consisted of taking sufficient measurements to permit computation of the hydraulic losses. The three types of branches which were tested are shown in figure 6. The tests were undertaken principally to determine the behavior of a new type of branch (the vaned-Y) by comparison with the standard types. This comparison is given in figure 7. The losses expressed in percent of the velocity head at section 1, which is just upstream from the branch, are plotted against percent of flow diverted through the branch. These losses were computed from the pressure measurements as follows:

$$\text{Loss of head} = \left(H_1 + \frac{V_1^2}{2g}\right) - \left(H_2 + \frac{V_2^2}{2g}\right)$$

where

H_1 = pressure head measured at section 1.

H_2 = pressure head measured at section 2.

V_1 = average velocity at section 1 = $\frac{Q_1}{A_1}$.

V_2 = average velocity at section 2 = $\frac{Q_2}{A_2}$.

The discharges Q_1 and Q_2 were obtained from the discharges measured with the V-notch (Q_1) and with the end orifice (Q_2). The loss computed as above was then corrected by subtracting the friction loss in the length from sections 1 to 2. The coefficient used to compute the friction loss was determined from measurements of loss from section 3 to the section just ahead of the end orifice. This run of pipe is long enough and sufficiently removed downstream to give a fair value for the friction coefficient.

It is evident from figure 8 that at zero diversion the three types are quite similar. The straight and conical Y's are slightly superior.

At the extreme of 100 percent diversion the conical Y is definitely superior to the other two. This branch is recommended for installation at Green Mountain because, in addition to a low loss at 0 percent diversion, it has the minimum loss at 100 percent. Thus it will affect the turbine efficiency only very slightly and will enable the needle valves to discharge more water for any given size. The values of loss for sections 1 to 2 at 100 percent diversion and for sections 1 to 4 at 0 percent diversion are meaningless, since there is no flow between the sections. Any loss computed from the pressure measurements is due either to secondary flow or errors in the measurements, and when this loss is expressed in terms of zero velocity head, the value goes to infinity.

Attention is called to the marked change in the performance of the vaned-Y, depending on whether the upstream edge of the Y is sharp or rounded. The sharp edge is definitely superior. The following condition observed in the model serves to explain this difference. At zero diversion there was a noticeable flow into the branch at the upstream edge and out of the branch at the downstream edge. This flow interferes with the main flow and causes additional loss. The cause of this flow is the pressure gradient across the opening of the branch, and when the upstream edge is rounded there is less resistance against the formation of this secondary flow.

Pressure measurements were taken at numerous points in the vaned-Y and these data are shown in figures 8 and 9.

The method used for computing the loss due to the Y-branch is only approximate in that it does not take into account the excess loss in the pipe downstream from the branch. However, for comparative purposes it is felt that this method is acceptable. The better but more complicated method of computing the losses was carried through for the condition of zero diversion. The results are shown as follows.

Assuming that the coefficient of frictional loss from section 1 to orifice is equal to 0.020, the computed loss is

$$h_f = 0.020 \times 15.62 \times \frac{V^2}{2g} = 0.312 \frac{V^2}{2g}$$

Y-branch	Measured Loss(ft.)	$\frac{V^2}{2g}$	Computed Loss(ft.)	Difference Feet	Difference % $\frac{V^2}{2g}$	
straight	0.330	0.700	0.218	0.112	16.0	mean 15.2
straight	0.335	0.723	0.226	0.109	15.1	
straight	0.330	0.723	0.226	0.104	14.4	
conical	0.335	0.725	0.226	0.109	15.0	
vaned(round)	0.355	0.614	0.192	0.163	26.5	
vaned(sharp)	0.325	0.683	0.213	0.112	16.4	

FIGURE 1

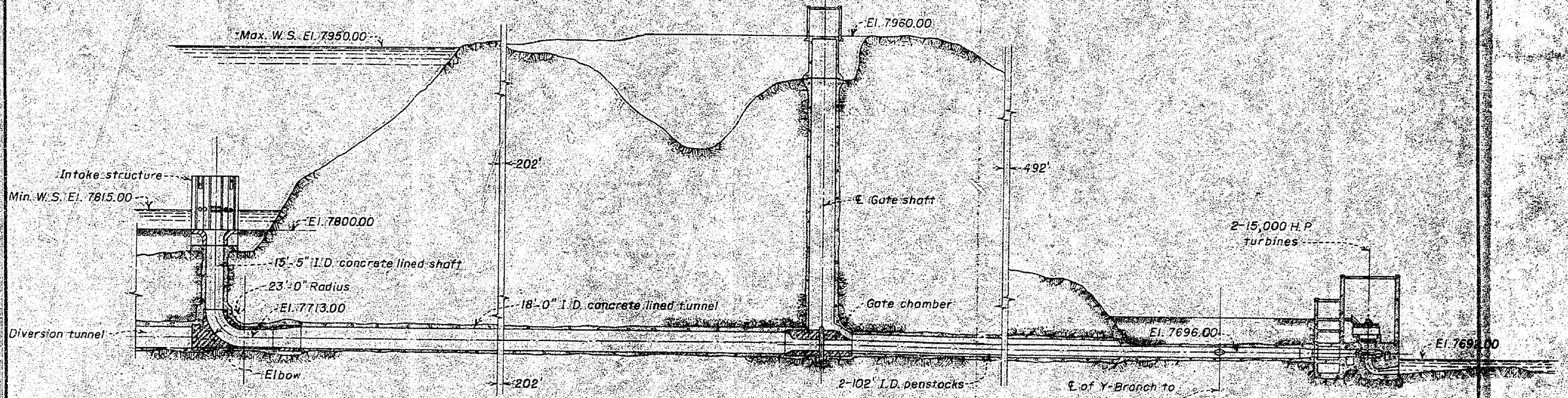

PROFILE ON ℄ OF OUTLET TUNNEL

50 0 50 100
SCALE OF FEET

GREEN MOUNTAIN PENSTOCK STUDIES
PRINCIPAL FEATURES OF PENSTOCK SYSTEM

FIGURE 1

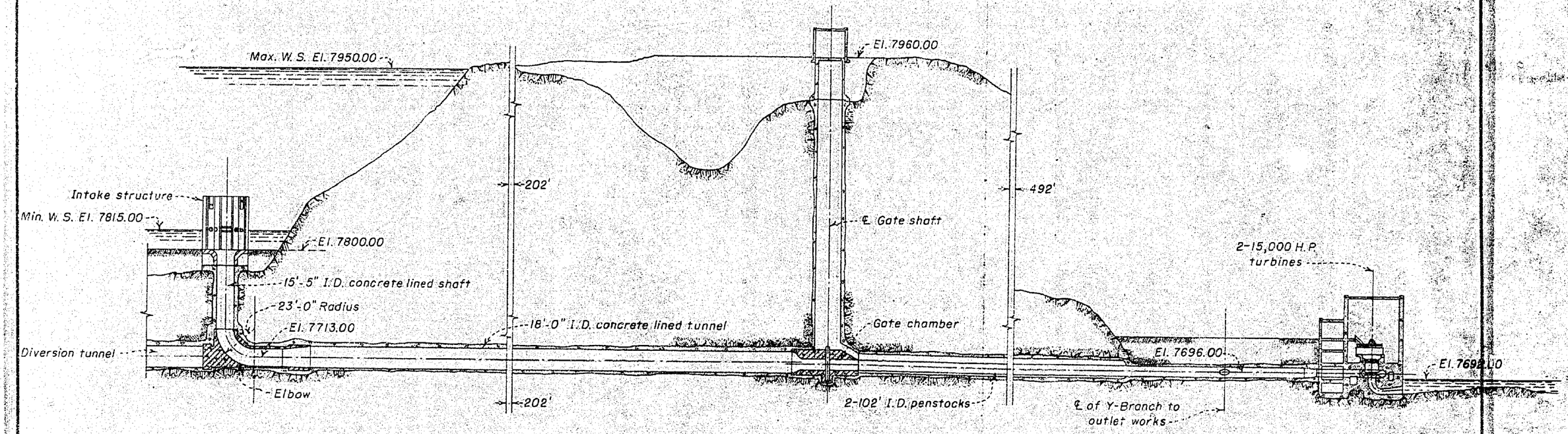

PROFILE ON ℄ OF OUTLET TUNNEL

50 0 50 100
SCALE OF FEET

GREEN MOUNTAIN PENSTOCK STUDIES
PRINCIPAL FEATURES OF PENSTOCK SYSTEM

FIGURE 2

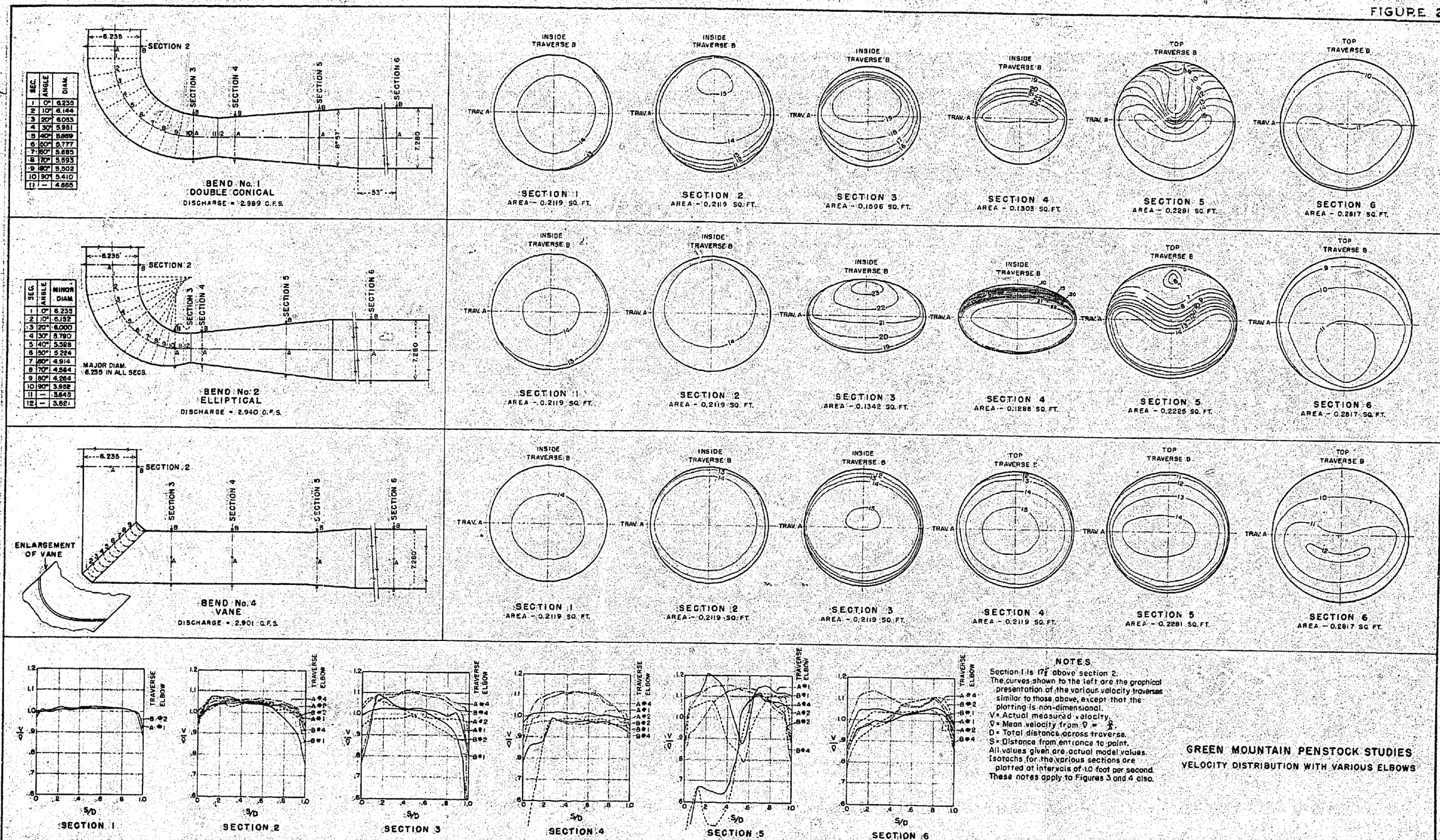

SEC.	ANGLE	DIAM.
1	0°	6.235
2	10°	6.144
3	20°	6.053
4	30°	5.961
5	40°	5.869
6	50°	5.777
7	60°	5.685
8	70°	5.593
9	80°	5.502
10	90°	5.410
11	—	4.865

SEC.	ANGLE	MINOR DIAM.
1	0°	6.235
2	10°	6.152
3	20°	6.000
4	30°	5.790
5	40°	5.525
6	50°	5.224
7	60°	4.914
8	70°	4.584
9	80°	4.264
10	90°	3.952
11	—	3.648
12	—	3.621

NOTES

Section 1 is 17½" above section 2.
The curves shown to the left are the graphical presentation of the various velocity traverses similar to those above, except that the plotting is non-dimensional.
V = Actual measured velocity.
V̄ = Mean velocity from $\bar{V} = \frac{Q}{A}$.
D = Total distance across traverse.
S = Distance from entrance to point.
All values given are actual model values.
Isotachs for the various sections are plotted at intervals of 1.0 foot per second.
These notes apply to Figures 3 and 4 also.

GREEN MOUNTAIN PENSTOCK STUDIES

VELOCITY DISTRIBUTION WITH VARIOUS ELBOWS

FIGURE 3

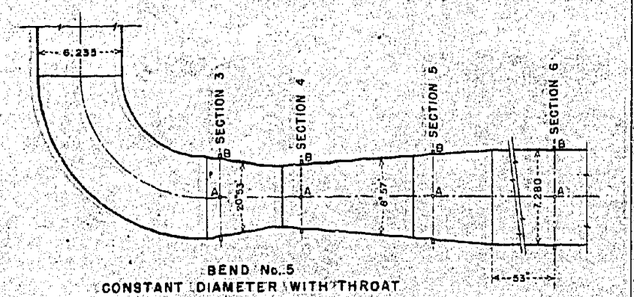

BEND No. 5
CONSTANT DIAMETER WITH THROAT
DISCHARGE = 13.018 C.F.S.

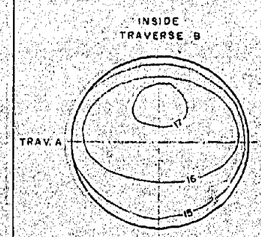

SECTION 3
AREA = 0.1862 SQ. FT.

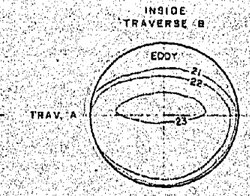

SECTION 4
AREA = 0.1303 SQ. FT.

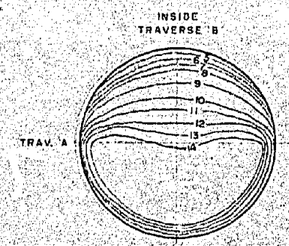

SECTION 5
AREA = 0.2281 SQ. FT.

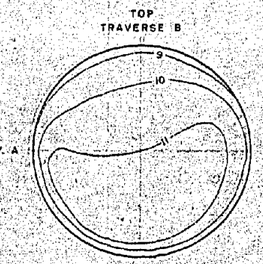

SECTION 6
AREA = 0.2817 SQ. FT.

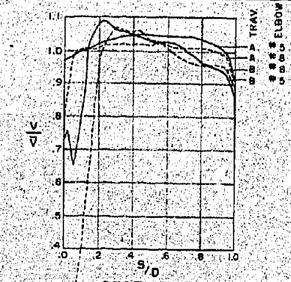

SECTION 3

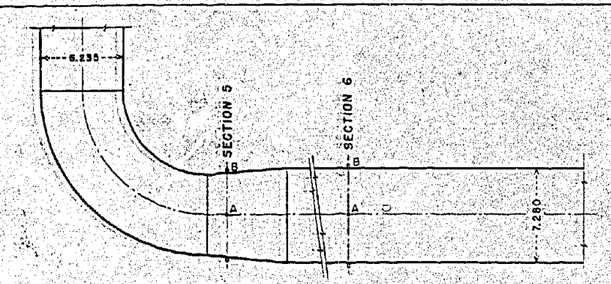

BEND No. 6
CONSTANT DIAMETER WITHOUT THROAT
DISCHARGE = 2.982 C.F.S.

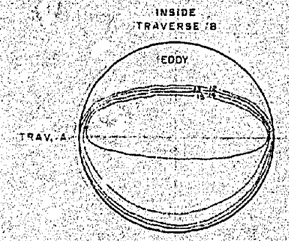

SECTION 5
AREA = 0.2281 SQ. FT.

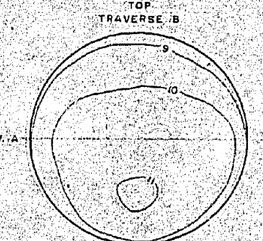

SECTION 6
AREA = 0.2817 SQ. FT.

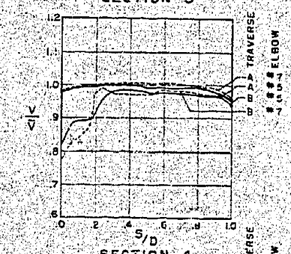

SECTION 4

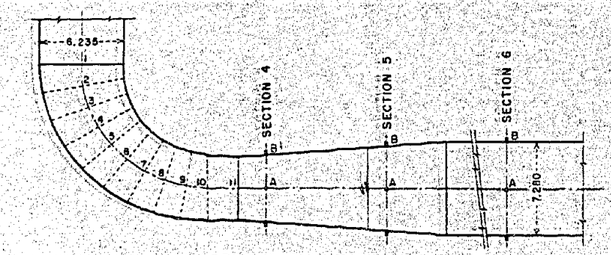

BEND No. 7
SINGLE CONICAL
DISCHARGE = 2.988 C.F.S.

SECTION	ANGLE	DIAM.
1	0°	6.235
2	10	6.087
3	20°	5.937
4	30°	5.738
5	40°	5.635
6	50°	5.485
7	60°	5.335
8	70°	5.190
9	80°	5.040
10	90°	4.890
11	—	4.685

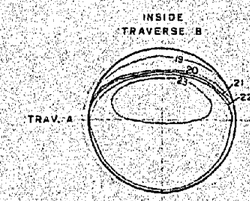

SECTION 4
AREA = 0.1303 SQ. FT.

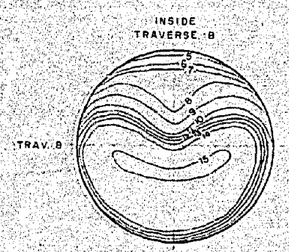

SECTION 5
AREA = 0.2281 SQ. FT.

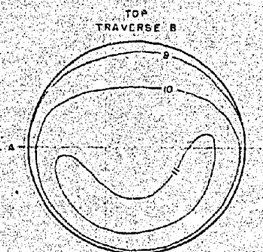

SECTION 6
AREA = 0.2817 SQ. FT.

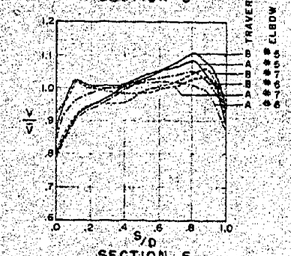

SECTION 5

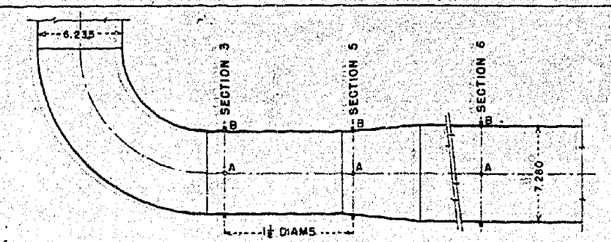

BEND No. 8
CONSTANT DIAMETER WITH 1½ D. STRAIGHT PIPE
DISCHARGE = 3.077 C.F.S.

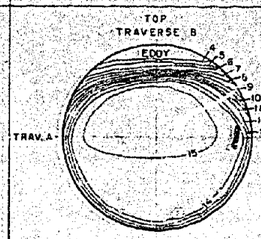

SECTION 3
AREA = 0.2119 SQ. FT.

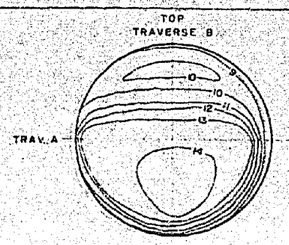

SECTION 5
AREA = 0.2281 SQ. FT.

NOTE
No traverses taken at Section 6.

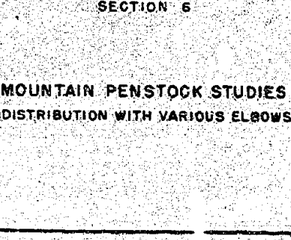

SECTION 6

GREEN MOUNTAIN PENSTOCK STUDIES
VELOCITY DISTRIBUTION WITH VARIOUS ELBOWS

HYD-95

FIGURE 4

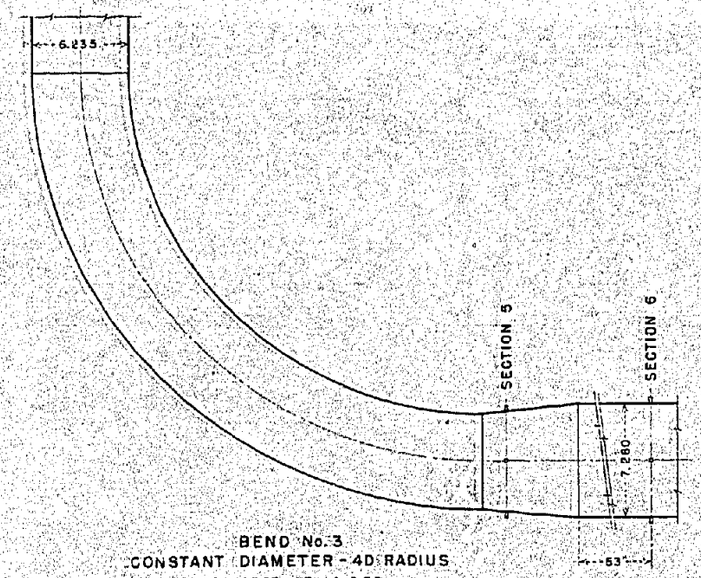

BEND No. 3
CONSTANT DIAMETER - 4D RADIUS
DISCHARGE = 3.114 C.F.S.

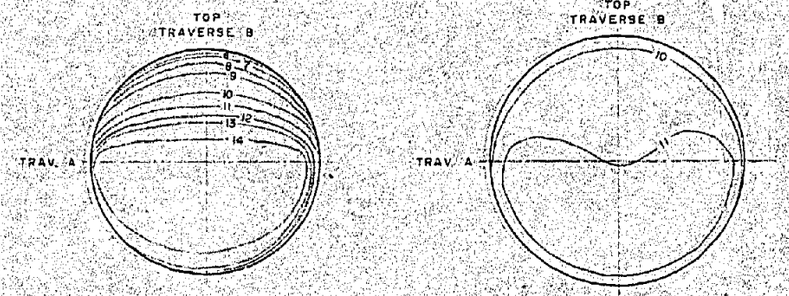

SECTION 5
AREA - 0.2281 SQ. FT.

SECTION 6
AREA - 0.2317 SQ. FT.

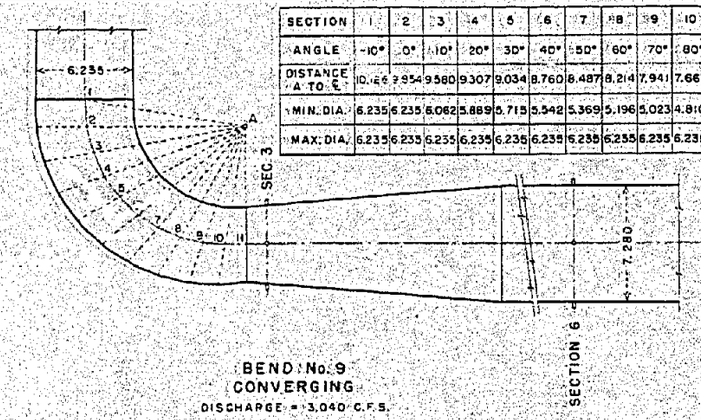

BEND No. 9
CONVERGING
DISCHARGE = 3.040 C.F.S.

SECTION	1	2	3	4	5	6	7	8	9	10	11
ANGLE	-10°	0°	10°	20°	30°	40°	50°	60°	70°	80°	90°
DISTANCE A TO ℄	10.466	9.954	9.580	9.307	9.034	8.760	8.487	8.214	7.941	7.667	7.543
MIN. DIA.	6.235	6.235	6.062	5.889	5.715	5.542	5.369	5.196	5.023	4.810	4.670
MAX. DIA.	6.235	6.235	6.235	6.235	6.235	6.235	6.235	6.235	6.235	6.235	6.235

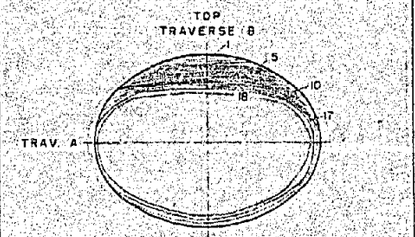

SECTION 3
AREA - 0.1676 SQ. FT.

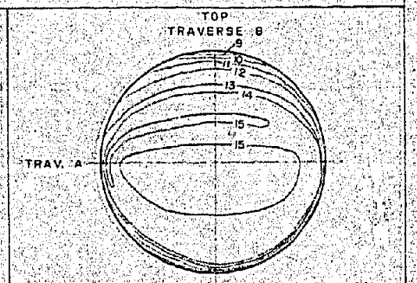

SECTION 3
AREA - 0.2119 SQ. FT.

BEND No. 4A
Same as bend No. 4 with vanes 2, 4, 6, and 8 removed.
DISCHARGE = 0.2972 C.F.S.

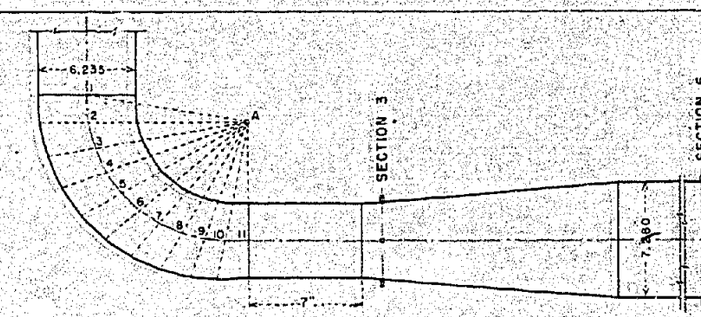

BEND No. 9A
CONVERGING WITH 7" D. STRAIGHT PIPE
DISCHARGE = 3.000 C.F.S.

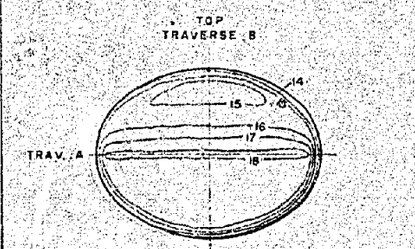

SECTION 3
AREA - 0.1676 SQ. FT.

NOTE
No traverses taken at Section 6 for bends 9 and 9A.

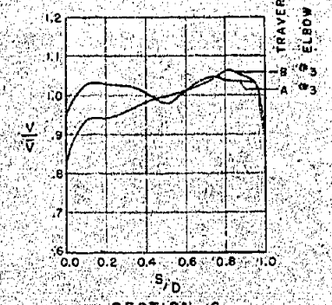

SECTION 6

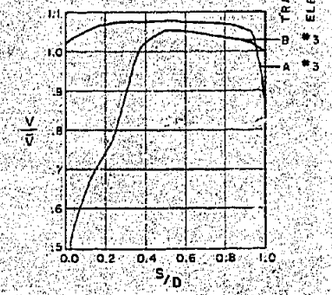

SECTION 5

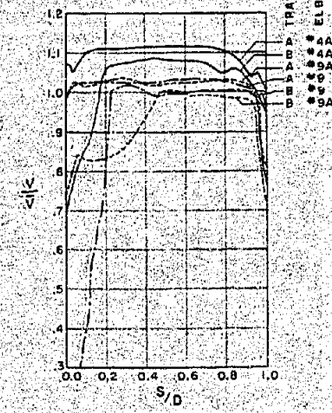

SECTION 3

GREEN MOUNTAIN PENSTOCK STUDIES
VELOCITY DISTRIBUTION WITH VARIOUS ELBOWS

FIGURE 5

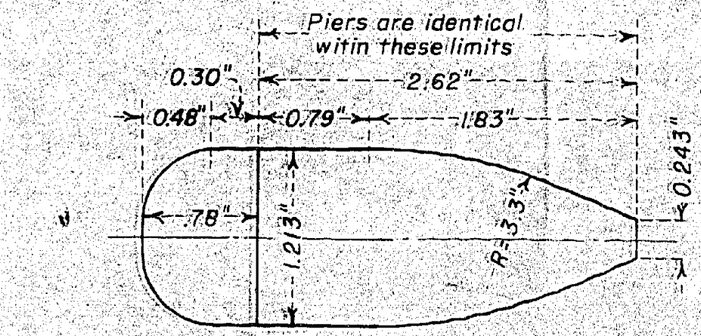

BLUNT

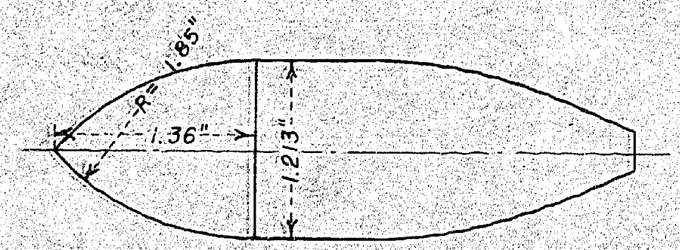

SHARP

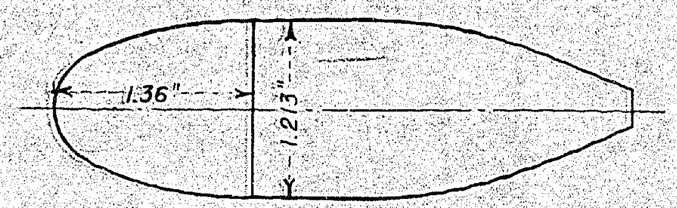

ELLIPTICAL
PIER SHAPES

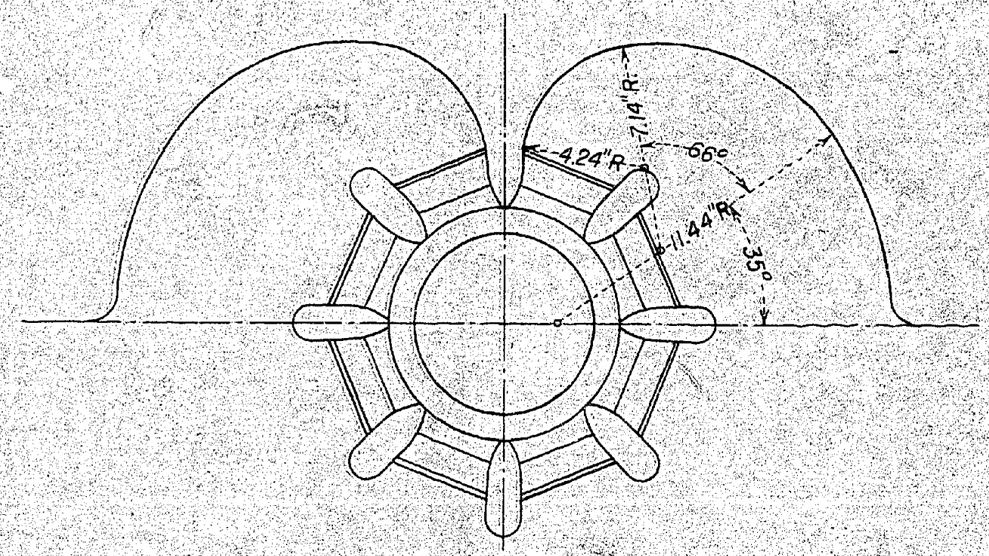

TRASHRACK AND TRAINING WALL

GREEN MOUNTAIN PENSTOCK STUDIES

FIGURE 6

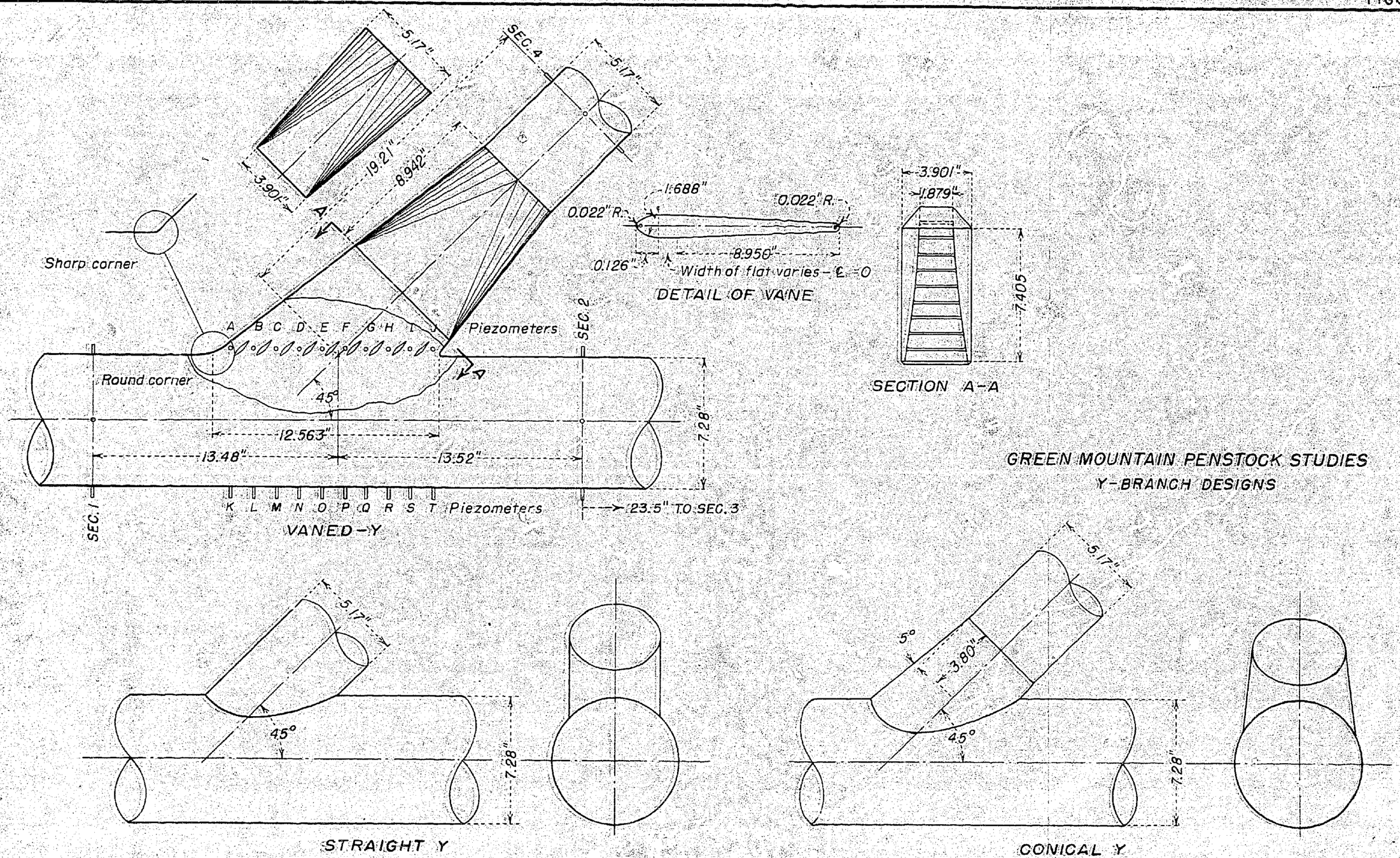

GREEN MOUNTAIN PENSTOCK STUDIES

Y-BRANCH DESIGNS

FIGURE 7

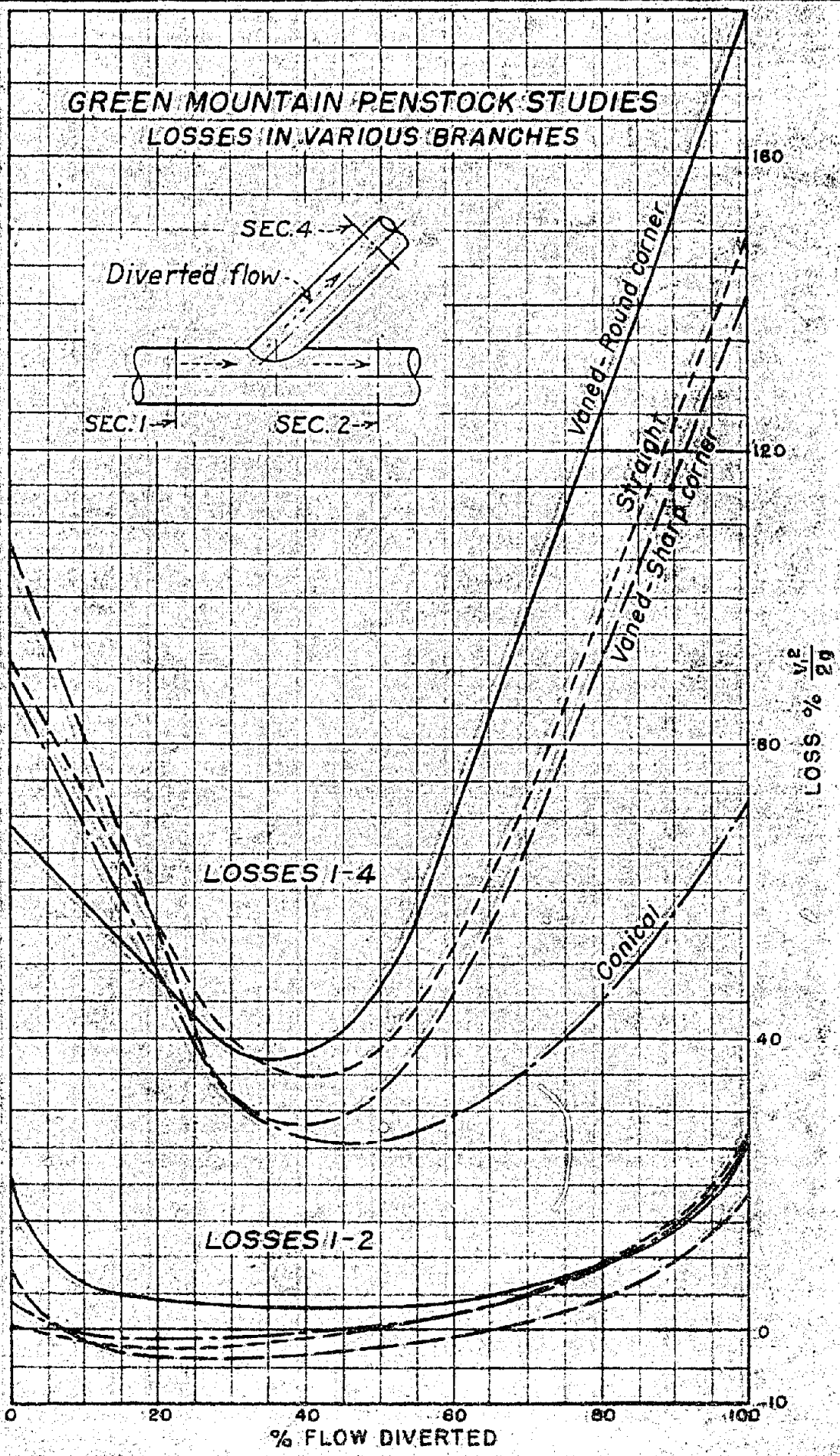
GREEN MOUNTAIN PENSTOCK STUDIES
LOSSES IN VARIOUS BRANCHES
SEC. 4
Diverted flow
SEC. 1
SEC. 2
Vaned-Round corner
Straight
Vaned-Sharp corner
Conical
LOSSES 1-4
LOSSES 1-2
160
120
80
40
0
-10
0
20
40
60
80
100
% FLOW DIVERTED
LOSS % $\frac{V^2}{2g}$

Table 1

Pressures in vaned-Y, round corner, in feet of water above center line of pipe.

X------Sections-----X				X---------Piezometers in branch flow---------X									X----------Piezometers in direct flow----------X										
1	2	3	4	A	B	C	D	E	F	G	H	I	J	K	L	M	N	O	P	Q	R	S	T
Q_t (total) = 1.065 c.f.s.; Q_d (direct) = 0.000 c.f.s.; Q_b (branch) = 1.065 c.f.s.; % diverted = 100																							
3.38	3.73	3.76	1.03	1.61	0.65	0.68	1.10	1.50	1.40	1.35	1.20	1.40	1.65	3.45	3.49	3.55	3.60	3.64	3.65	3.66	3.66	3.65	3.65
Q_t = 2.226 c.f.s.; Q_d = 0.667 c.f.s.; Q_b = 1.559 c.f.s.; % diverted = 70.1																							
2.16	2.90	2.95	1.47	0.63	$\overline{1}$.15	$\overline{0}$.97	$\overline{0}$.71	0.22	0.78	0.82	0.96	1.10	1.20	2.30	2.36	2.42	2.50	2.60	2.69	2.76	2.81	2.83	2.85
Q_t = 1.466 c.f.s.; Q_d = 0.721 c.f.s.; Q_b = 0.745 c.f.s.; % diverted = 50.8																							
3.34	3.60	3.60	3.14	2.93	2.55	2.71	2.86	2.87	2.98	3.03	3.12	3.19	3.35	3.38	3.40	3.42	3.44	3.47	3.50	3.51	3.53	3.54	3.56
Q_t = 2.428 c.f.s.; Q_d = 0.680 c.f.s.; Q_b = 1.748 c.f.s.; % diverted = 72.1																							
2.10	3.01	3.08	$\overline{0}$.02	0.44	$\overline{1}$.55	$\overline{1}$.40	$\overline{1}$.07	0.90	$\overline{0}$.87	0.27	0.43	0.70	0.75	2.27	2.37	2.45	2.53	2.65	2.75	2.82	2.86	2.91	2.93
Q_t = 2.870 c.f.s.; Q_d = 1.581 c.f.s.; Q_b = 1.289 c.f.s.; % diverted = 44.9																							
0.57	1.52	1.46	0.31	$\overline{0}$.78	$\overline{1}$.90	$\overline{1}$.16	$\overline{0}$.66	$\overline{0}$.24	0.01	0.17	0.30	0.22	0.72	0.68	0.79	0.85	0.90	1.03	1.13	1.20	1.28	1.35	1.40
Q_t = 2.551 c.f.s.; Q_d = 1.820 c.f.s.; Q_b = 0.731 c.f.s.; % diverted = 28.6																							
1.84	2.40	2.24	2.27	1.11	0.65	1.22	1.52	1.81	2.00	2.03	2.11	2.16	2.15	1.94	2.01	2.05	2.07	2.16	2.22	2.24	2.30	2.32	2.35
Q_t = 2.255 c.f.s.; Q_d = 1.916 c.f.s.; Q_b = 0.339 c.f.s.; % diverted = 15.0																							
2.58	2.76	2.59	3.09	2.16	1.92	2.28	2.49	2.73	2.84	2.81	2.93	2.96	2.85	2.63	2.68	2.70	2.60	2.75	2.77	2.76	2.80	2.79	2.78
Q_t = 1.927 c.f.s.; Q_d = 1.929 c.f.s.; Q_b = 0.000 c.f.s.; % diverted = 0.0																							
2.94	2.78	2.62	3.17	2.93	2.85	2.96	2.97	3.03	3.13	3.05	3.09	3.03	2.83	2.95	2.97	2.97	2.94	2.98	2.96	2.93	2.93	2.90	2.87

Figure 8

Fig. 8

Table 2

Pressures in vaned-Y, sharp corner, in feet of water above center line of pipe.

X------Sections-----X																							
				X---------Piezometers in branch flow---------X								X----------Piezometers in direct flow----------X											
1	2	3	4	A	B	C	D	E	F	G	H	I	J	K	L	M	N	O	P	Q	R	S	T
Q_t (total) = 1.916 c.f.s.; Q_d (direct) = 1.916 c.f.s.; Q_b (branch) = 0.000 c.f.s.; % diverted = 0.0																							
2.88	2.80	2.62	2.88	2.89	2.83	2.86	2.85	2.85	2.84	2.83	2.82	2.82	2.80	2.85	2.86	2.86	2.82	2.84	2.84	2.82	2.83	2.82	2.81
Q_t = 2.533 c.f.s.; Q_d = 1.865 c.f.s.; Q_b = 0.668 c.f.s.; % diverted = 26.3																							
2.02	2.55	2.38	2.18	1.75	1.70	1.71	1.59	1.54	1.50	1.69	1.70	1.72	1.74	2.06	2.12	2.13	2.13	2.22	2.28	2.32	2.39	2.43	2.47
Q_t = 2.724 c.f.s.; Q_d = 1.819 c.f.s.; Q_b = 0.905 c.f.s.; % diverted = 33.2																							
1.64	2.37	2.22	1.92	0.31	0.10	0.80	1.21	1.47	1.62	1.72	1.79	1.81	1.73	1.72	1.81	1.85	1.88	1.99	2.07	2.11	2.19	2.23	2.27
Q_t = 2.870 c.f.s.; Q_d = 1.694 c.f.s.; Q_b = 1.176 c.f.s.; % diverted = 41.0																							
1.05	1.94	1.84	1.08	$\overline{0}.42$	$\overline{0}.96$	$\overline{0}.22$	0.26	0.62	0.89	1.05	1.15	1.11	1.27	1.24	1.35	1.41	1.44	1.57	1.67	1.73	1.82	1.87	1.91
Q_t = 1.288 c.f.s.; Q_d = 0.741 c.f.s.; Q_b = 0.547 c.f.s.; % diverted = 42.5																							
3.68	3.87	3.86	3.66	3.37	3.24	3.39	3.49	3.56	3.62	3.65	3.67	3.62	3.72	3.72	3.74	3.67	3.77	3.79	3.81	3.82	3.84	3.85	3.86
Q_t = 1.544 c.f.s.; Q_d = 0.726 c.f.s.; Q_b = 0.818 c.f.s.; % diverted = 53.0																							
3.36	3.67	3.68	3.10	2.79	2.41	2.60	2.66	2.74	2.83	2.96	3.09	3.17	3.30	3.39	3.43	3.46	3.48	3.51	3.53	3.56	3.58	3.60	3.62
Q_t = 1.906 c.f.s.; Q_d = 0.718 c.f.s.; Q_b = 1.188 c.f.s.; % diverted = 61.8																							
2.97	3.54	3.56	2.18	2.00	0.98	1.12	1.24	1.82	1.96	2.24	2.36	2.48	2.60	3.06	3.11	3.15	3.19	3.25	3.30	3.33	3.37	3.41	3.44
Q_t = 2.434 c.f.s.; Q_d = 0.684 c.f.s.; Q_b = 1.750 c.f.s.; % diverted = 71.9																							
2.12	3.05	3.14	0.01	0.09	$\overline{2}.13$	$\overline{1}.68$	$\overline{1}.42$	$\overline{0}.05$	0.06	0.46	0.53	0.73	0.89	2.29	2.39	2.48	2.56	2.69	2.80	2.87	2.93	2.94	2.96
Q_t = 1.610 c.f.s.; Q_d = 0.000 c.f.s.; Q_b = 1.610 c.f.s.; % diverted = 100.0																							
3.43	3.80	3.84	1.18	1.69	0.62	0.63	1.04	1.53	1.46	1.26	1.24	1.62	1.90	3.55	3.61	3.67	3.71	3.74	3.76	3.77	3.78	3.78	3.78

Figure 9

DETAILS OF GREEN MOUNTAIN PENSTOCK MODEL

INTAKE STRUCTURE

ELBOW

Y BRANCH